



**HAL**  
open science

## Organ-wide and ploidy-dependent regulations both contribute to cell size determination: evidence from a computational model of tomato fruit

Valentina Baldazzi, Pierre Valsesia, Michel Génard, Nadia Bertin

### ► To cite this version:

Valentina Baldazzi, Pierre Valsesia, Michel Génard, Nadia Bertin. Organ-wide and ploidy-dependent regulations both contribute to cell size determination: evidence from a computational model of tomato fruit. 2018. hal-01953178

**HAL Id: hal-01953178**

**<https://inria.hal.science/hal-01953178v1>**

Preprint submitted on 12 Dec 2018

**HAL** is a multi-disciplinary open access archive for the deposit and dissemination of scientific research documents, whether they are published or not. The documents may come from teaching and research institutions in France or abroad, or from public or private research centers.

L'archive ouverte pluridisciplinaire **HAL**, est destinée au dépôt et à la diffusion de documents scientifiques de niveau recherche, publiés ou non, émanant des établissements d'enseignement et de recherche français ou étrangers, des laboratoires publics ou privés.

1 **Organ-wide and ploidy-dependent regulations both contribute to cell size**  
2 **determination: evidence from a computational model of tomato fruit**

3 Valentina Baldazzi<sup>1,2,3</sup>, Pierre Valsesia<sup>1</sup>, Michel Génard<sup>1</sup>, Nadia Bertin<sup>1</sup>

4

5<sup>1</sup>INRA, PSH, France

6<sup>2</sup>Université Côte d'Azur, INRA, CNRS, ISA, France

7<sup>3</sup> Université Côte d'Azur, Inria, INRA, CNRS, UPMC Univ Paris 06, BIOCORE,  
8 France

9

10

11 **Abstract**

12

13 **The development of a new organ is the result of coordinated events of cell**  
14 **division and expansion, in strong interaction with each other. This paper**  
15 **presents a dynamic model of tomato fruit development that includes cells**  
16 **division, endoreduplication and expansion processes. The model is used to**  
17 **investigate the interaction among these developmental processes, in the**  
18 **perspective of a neo-cellular theory. In particular, different control schemes**  
19 **(either cell-autonomous or organ-controlled) are tested and results**  
20 **compared to observed data from two contrasted genotypes. The model**  
21 **shows that a pure cell-autonomous control fails to reproduce the observed**  
22 **cell size distribution, and an organ-wide control is required in order to get**  
23 **realistic cell sizes. The model also supports the role of endoreduplication**  
24 **as an important determinant of the final cell size and suggests a possible**  
25 **interaction through carbon allocation and metabolism.**

26

27 **Keywords:** cell size, division, development, expansion, endoreduplication,  
28 growth, model, ploidy, tomato

29

30 **INTRODUCTION**

31 Understanding the mechanisms underpinning fruit development from its  
32 early stages is of primary importance for biology and agronomy. Indeed, early  
33 stages are highly sensitive to biotic and abiotic stresses, with important

34consequences on fruit set and yield. The development of a new organ is the  
35result of coordinated events of cell division and expansion. Fruit growth starts  
36immediately after pollination with intensive cell division. As development  
37proceeds, the proliferative activity of cells progressively slows down giving way to  
38a phase of pure cell enlargement during fruit growth and ripening. In many  
39species, including tomato, the transition from cell division to expansion phases is  
40accompanied by repeated DNA duplications without mitosis, a process called  
41endoreduplication. The exact role of endoreduplication is still unclear. A strong  
42correlation between cell ploidy (i.e number of DNA copies) and final cell size has  
43been observed in different species (Bertin, 2005; Lee et al., 2007; Melaragno et  
44al., 1993; Rewers et al., 2009), suggesting a role of endoreduplication into the  
45control of organ growth (Breuer et al., 2010; Chevalier et al., 2011).

46 Understanding the way cell division, endoreduplication and expansion  
47processes interact is crucial to predict the emergence of important morphological  
48traits (fruit size, mass, shape and texture) and their dependence on  
49environmental and genetic factors. Historically, a big debate has opposed two  
50contrasting views, the cellular vs the organismal theory that set the control of  
51organ growth at the level of the individual cell or of the whole tissue, respectively  
52(reviewed in (Beemster et al., 2003; Fleming, 2006; John and Qi, 2008). In the  
53recent years, a consensus view, the neo-cellular theory, has eventually emerged.  
54Accordingly, although individual cells are the units of plant morphology, their  
55behavior (division, expansion) is not autonomous, but coordinated at the organ  
56level by cell-to-cell communication mechanisms, thus creating an effective  
57interaction between cellular and whole-organ behavior (Beemster et al., 2003;  
58Sablowski and Carnier Dornelas, 2014; Tsukaya, 2003). The existence of non-cell  
59autonomous control of organ development has been demonstrated in *Arabidopsis*  
60leaf (Kawade et al., 2010) but the underlying modes of action remain unclear  
61and often system-specific (Ferjani et al., 2007; Han et al., 2014; Horiguchi and  
62Tsukaya, 2011; Norman et al., 2011; Okello et al., 2015).

63

64Computational models offer a unique tool to express and test biological  
65hypotheses, in a well-defined and controlled manner. Not surprisingly, indeed,  
66computational modeling has been largely used to investigate the relationships  
67between organ development and the underlying cellular processes. Many works  
68have addressed the question of organogenesis, relating local morphogenetic  
69rules and cell mechanical properties with the emerging patterns near the  
70meristem (Boudon et al., 2015; Dupuy et al., 2010; Kuchen et al., 2012; Löffke  
71et al., 2015; Lucas et al., 2013; Robinson et al., 2011) (von Wangenheim et al.,  
722016). At the tissue scale, a few models have addressed the issue of cell's size  
73variance based on observed kinematic patterns of cell division or growth rates,  
74with a particular attention to the intrinsic stochasticity of cell-cycle related  
75processes (Asl et al., 2011; Kawade and Tsukaya, 2017; Roeder et al., 2010). In  
76most of these models, cell expansion is simply described via an average growth  
77rate, possibly modulated by the ploidy level of the cell, without any reference to  
78the underlying molecular mechanisms or to the environmental conditions.

79

80 To our knowledge, very few attempts have been made to explicitly model  
81the interaction among cell division, expansion and endoreduplication from first  
82principles and at the scale of organ development. In Fanwoua et al., 2013 a  
83model of tomato fruit development have been developed that integrates cell  
84division, expansion and endoreduplication processes based on a set of  
85biologically-inspired rules. The fruit is described by a set of  $q$  classes of cells with  
86the same age, ploidy and mass. Within each class, cell division and  
87endoreduplication are described as discrete events that take place within a well-  
88defined window of time, whenever a specific mass-to-ploidy threshold is reached.  
89Cell growth in dry mass is modeled following a source-sink approach as a  
90function of the thermal time, the cell ploidy-level and the external resources. The  
91model is able to qualitatively capture the effect of environmental conditions  
92(temperature, fruit load) on the final fruit dry mass, but hypotheses and  
93parameters are hard to validate as comparison to experimental data is lacking.  
94Moreover, the water content of the cell is not considered preventing the analysis

95of cell volumes.

96       Baldazzi and coworkers developed an integrated model of tomato fruit  
97development which explicitly accounts for the dynamics of cell proliferation as  
98well as for the mechanisms of cell expansion, in both dry and fresh masses,  
99based on biophysical and thermodynamical principles (Baldazzi et al., 2012,  
1002013). Here, a new version of this model, which includes cell endoreduplication,  
101is proposed. The model was used to investigate different hypotheses concerning  
102the regulation and the interaction among cellular processes, with special attention  
103to 1) the importance of an organ-wide regulation on cell growth and 2) the  
104mechanisms of interaction between endoreduplication and cell expansion  
105processes.

106We focus on a natural, wild type organ development and we analyze the effect of  
107organ-wide or cell ploidy-dependent regulation onto the dynamics of cell  
108expansion. To this aim, different control schemes (either cell-autonomous or  
109organ-controlled, with or without ploidy effect on cell expansion) were tested *in*  
110*silico* by means of specific model variants. Simulation results were analyzed and  
111compared to cell size distributions observed on two contrasted genotypes, a  
112cherry and a large-fruited tomato variety.

113The model shows that a pure cell-based control cannot reproduce the observed  
114cell size distribution, and an organ-wide control is required in order to get realistic  
115cell and fruit sizes. The model also supports the role of endoreduplication as an  
116important modulator of the cell expansion potential, although the strength of this  
117interaction might be genotype-specific. In particular, results suggest a likely  
118interaction through carbon allocation and metabolism.

119

120

## 121**MATERIALS AND METHODS**

122

### 123**Experimental data**

124

125Two datasets were collected from two glasshouse experiments performed at

126INRA Avignon (south of France) in 2004 and 2007 on large-fruited (cv Levovil)  
127and cherry (cv. Cervil) tomato genotypes of *Solanum lycopersicum* L.  
128  
129The 2004 experiment fruits were collected from April to May (planting in February)  
130whereas in the 2007 experiment fruits were sampled from October to December  
131(planting in August). Plants were grown according to standard cultural practices.  
132Trusses were pruned in order to homogenise truss size along the stem within  
133each genotype. Maximum number of flowers left on each inflorescence was 12  
134for Cervil and 6 for Levovil. Flowers were pollinated by bumblebees. Air  
135temperature and humidity were recorded hourly in each experiment and input in  
136the model as external signals.  
137Flower buds and fruits were sampled at different time points relative to the time of  
138flower anthesis (full-flower opening). Fruit fresh and dry mass and pericarp fresh  
139mass were systematically measured at all times points, before further  
140measurements. In 2004, half of the fruit pericarps were then analyzed by flow  
141cytometry and the other half were used for the determination of cell number. The  
142number of pericarp cells was measured after tissue dissociation according to a  
143method adapted from that of Bünger-Kibler and Bangerth, 1982 and detailed in  
144(Bertin et al., 2003). Cells were counted in aliquots of the cell suspension under  
145an optical microscope, using Fuchs-Rosenthal chambers or Bürker chambers for  
146the large and small fruits, respectively. Six to 8 aliquots per fruits were observed  
147and the whole pericarp cell number was calculated according to dilution and  
148observation volumes. The ploidy was measured in the pericarp tissue, as  
149described in Bertin et al., 2007. The average value of three measurements per  
150fruit (when allowed for by the fruit's size), was included in the analysis.  
151  
152In the 2007 experiment, the dynamics of cell number (but not endoreduplication)  
153was measured following the same method as in the 2004 experiment. In addition,  
154cell size distribution (smallest and largest radii and 2D-surface) distributions were  
155measured with ImageJ software ([imagej.nih.gov/ij/](http://imagej.nih.gov/ij/)) in the cell suspension  
156aliquots. About 20 to 25 cells per fruit were measured randomly on different  
157fruits. Cell size distribution were derived for ripe fruits at about 43 days after

158anthesis (DAA) for Cervil and 60 DAA for Levovil in the considered growing  
159conditions.

160

161

## 162**Model description**

163

164 The model is composed of two interacting modules, both issued from  
165previously published models (Bertin et al., 2007; Fishman and Génard, 1998; Liu  
166et al., 2007). The fruit is described as a collection of cell populations, each one  
167having a specific age, ploidy and volume, which evolve and grow over time during  
168fruit development. The number, age (initiation date) and physiological state  
169(proliferating or endoreduplicating-expanding cells) of each population is  
170predicted by the cell division-endoreduplication module (Bertin et al., 2007),  
171based on genotype-specific parameters. It is assumed that the onset of  
172endoreduplication coincides with the beginning of the expansion phase, i.e.  
173expanding cells are endoreduplicating.

174

175At any time, mass (both fresh and dry component) of expanding cells is computed  
176by a biophysical expansion module according to cell's characteristics (age,  
177ploidy) and depending on available resources and environmental conditions  
178(Fishman and Génard, 1998; Liu et al., 2007). Briefly, cell expansion is described  
179by iteratively solving the Lockhart equation relating the rate of volume increase to  
180the cell's internal pressure and cell's mechanical properties (Lockhart, 1965).  
181Flows of water and solutes across the membrane are described by  
182thermodynamic equations and depend on environmental conditions. The relative  
183importance of each transport process may vary along fruit developmental stages,  
184depending on specific developmental control. A full description of the model and  
185its equations can be found in the section S2 of the Supplemental Material.  
186In its standard version, the model assumes that all cells have equal access to  
187external resources, independently from the number of cells (no competition). All  
188the parameters of the division- endoreduplication module are considered to be  
189independent from environmental conditions for the time being.

190

191

## 192 **Model initialisation and input**

193

194 The model starts at the end of the division-only phase, when the  
195 proliferative activity of the cells declines and the expansion phase begins  
196 (Baldazzi et al., 2013). For Cervil genotype this corresponds to approximately 8  
197 days before anthesis and to 3 days before anthesis for Levovil genotype (Bertin  
198 et al., 2007). The initial number of cells,  $n_0$ , was estimated to  $1e4$  for the cherry  
199 tomato (Cervil) and  $1.8e5$  for the large-fruited (Levovil) genotype based on a few  
200 measurements.

201 At the beginning of the simulation, all cells are supposed to be proliferating  
202 with a ploidy level of 2C (transient ploidy of 4C during cell cycle is not  
203 considered). Proliferating cells are supposed to have a constant cell mass,  $m_0$ ,  
204 as often observed in meristematic cells (homogeneous/uniformity in cell size)  
205 (Sablowski and Carnier Dornelas, 2014; Serrano-Mislata et al., 2015). The initial  
206 mass of the fruit is therefore  $M_f(0) = n_0 * m_0 = n_0 * (w_0 + s_0)$ , where  $w_0$  and  $s_0$  are  
207 initial cell water and dry mass, respectively. At any time, cells leaving the  
208 proliferative phase start to grow, from an initial mass  $2 * m_0$  and a ploidy level of  
209 4C, according to the expansion model and current environmental conditions.

210

211 Cell expansion depends on environmental conditions and resources provided by  
212 the mother plant. The phloem sugar concentration is assumed to vary daily  
213 between 0.15 and 0.35 M whereas stem water potential oscillates between -0.05  
214 and -0.6 MPa i.e. typical pre-dawn and minimal stem water potential measured  
215 for the studied genotypes. Temperature and humidity are provided directly by  
216 real-time recording of greenhouse climatic conditions.

217

## 218 **Choice of the model variants: control of cell expansion capabilities**

219

220 In the integrated model, a number of time-dependent functions account for  
221 developmental regulation of cell's metabolism and physical properties during the

222expansion phase (Baldazzi et al. 2013, Liu et al. 2007 ). Two characteristic time-  
223scales are recognizable in the model: the *cell age*, i.e. the time spent since an  
224individual cell has left the proliferative phase, and *organ age* i.e. the time spent  
225since the beginning of the simulation (Figure 1). Depending on the settings of the  
226corresponding time-dependent functions, different cellular processes may be put  
227under cell-autonomous or non-cell autonomous control (hereafter indicated as  
228organ-wide control), allowing for an *in silico* exploration of alternative control  
229hypotheses in the perspective of the cellular and organismal theories. Moreover,  
230a direct effect of cell DNA content onto cell expansion capabilities may be tested  
231according to biological evidences (Chevalier et al., 2011; Edgar et al., 2014;  
232Sugimoto-Shirasu and Roberts, 2003).

233

234As a default all cellular processes are supposed to be dependent on cell age  
235(cell-autonomous control) with the only exception of cell transpiration which is  
236computed at the organ scale, on the basis of fruit external surface and skin  
237conductance, and then distributed back to individual cells, proportionally to their  
238relative water content (see section S2).

239

240       Based on literature information and on preliminary tests ((Baldazzi et al.,  
2412013, 2017), the switch between symplastic and apoplastic transport,  $\sigma_p$  has  
242been selected as the candidate process for an organ-wide control. Indeed,  
243intercellular movement of macromolecules across plasmodesmata has been  
244shown to be restricted by organ age in tobacco leaves (Crawford and Zambryski,  
2452001; Zambryski, 2004) and it is known to be important for cell-to-cell  
246communication (Han et al., 2013).

247

248The exact mechanisms by which cell DNA content may affect cell expansion  
249remains currently unknown. Based on literature information and common sense,  
250three distinct mechanisms of interaction between endoreduplication and cell  
251expansion were hypothesized.

252

2531) Endoreduplication has been often associated to an elevated protein synthesis

254and transcriptional activity (Chevalier et al., 2014) suggesting a general activation  
 255of the nuclear and metabolic machinery of the cell to sustain cell growth  
 256(Sugimoto-Shirasu and Roberts, 2003). Following these insights, a first  
 257hypothesis assumes an effect of endoreduplication on cell expansion as a ploidy-  
 258dependent maximal import rate for carbon uptake. For sake of simplicity, the  
 259relation was supposed to be linear in the number of endocycles. The  
 260corresponding equation, as a function of the cell DNA content (DNA<sub>c</sub>, being 2 for  
 261dividing cells, 4 to 512 for endoreduplicating cells), was

262

$$263 \quad v_m = \langle v^0 \rangle * \log_2(DNA_c) \quad ,$$

264

265where  $\langle v^0 \rangle$  is the average C uptake activity per unit mass.

266

2672) In addition to a high transcriptional activity, endoreduplicating cells are  
 268characterized by a reduced surface-to-volume ratio with respect to 2C cells. As a  
 269consequence, it is tempting to speculate that one possible advantage of a high  
 270ploidy level may reside in a reduction of carbon demand for cell wall and  
 271structural units (Barow, 2006; Pirrello et al., 2018). Such an economy may impact  
 272cell expansion capabilities in two ways. First, the metabolic machinery could be  
 273redirected towards the synthesis of soluble components, thus contributing to the  
 274increase of cell's internal pressure and consequent volume expansion.  
 275In the model, the *ssrat* fraction of soluble compound within the cell is

276developmentally regulated by the age *t* of the cell (Baldazzi et al. 2013) as

277

$$278 \quad ssrat = b_{ssrat} (1 - e^{-a_{ssrat} * t}) + ssrat_0$$

279

280In the presence of a ploidy effect, the final *bssrat* value was further increased as

281

$$282 \quad b_{ssrat} = b_{ssrat}^0 * \log_2(DNA_c)$$

283

2843) Alternatively, “exceeding” carbon may be used to increase the rate of cell wall  
 285synthesis or related proteins, resulting in an increase of cell wall plasticity

286(Proseus and Boyer, 2006).

287

288In the original expansion model on tomato (Liu et al., 2007) cell wall extensibility

289Phi declines during cell maturation (Proseus et al., 1999) as  
290

$$291 \quad \Phi = \Phi_{min} + \frac{(\Phi_{max} - \Phi_{min})}{1 + e^{k(t - t_0)}}$$

292

293In the presence of a ploidy effect, the maximal cell wall extensibility was

294increased as

295

$$296 \quad \Phi_{max} = \Phi_{max}^0 * \log_2(DNAc)$$

297

298

299The individual and combined effects of organ-wide and ploidy-dependent control

300(one process at time) on cell expansion were investigated and compared to a full

301cell-autonomous model. A total of 8 model variants have been tested for each

302genotype, following the complete experimental design shown in Table 1.

303

#### 304**Model calibration**

305Calibration has been performed using genetic algorithm under R software (library

306'genalg'). A two-steps procedure has been used for each tomato genotype.

307First, the division-expansion module (7 parameters) was calibrated on data from

308the 2004 experiment by comparing measured and simulated values of the total

309cells number and the proportion of cells in different ploidy classes, all along fruit

310development. The best fitting parameters were selected and kept fixed for the

311second phase of the calibration, assuming they are independent from

312environmental conditions.

313The expansion module was calibrated on the evolution of pericarp fresh and dry

314mass from the 2007 experiment, for which cell size distribution were measured.

315Six parameters have been selected for calibration based on a previous sensitivity

316analysis (Constantinescu et al., 2016), whereas the others have been fixed to the

317original models' values (Baldazzi et al., 2013; Fishman and Génard, 1998; Liu et

318al., 2007). An additional parameter was estimated for model variants M3 to M7 in

319order to correctly evaluate the strength of the ploidy-dependent control (see

320section S3 for more information).

321Due to their different structures, the expansion module was calibrated  
322independently for each model variant. The quality of model adjustment was  
323evaluated using a Normalized Root Mean Square Error (NRMSE):

$$324 \quad NRMSE(x) = 100 \frac{\sqrt{\frac{1}{n} \sum (O_i - S_i(x))^2}}{\frac{1}{n} \sum O_i}$$

325

326where  $O_i$  and  $S_i$  are respectively, the observed and simulated values of pericarp  
327fresh and dry masses, and  $n$  is the number of observations.  $x = \{x_1, x_2 \dots x_p\}$  is  
328parameter set of the evaluated solution. The smaller the NRMSE the better the  
329goodness-of-fit is. A NRMSE < 20% is generally considered good, fair if 20% <  
330NRMSE < 30% and poor otherwise.

331To avoid high mean fitting errors in each condition, the choice of the best  
332calibration solution was based on a min-max decision criterion (Constantinescu et  
333al., 2016):

$$334 \quad \min_{x \in X} \left\{ \max \left( NRMSE_{FM}(x), NRMSE_{DM}(x) \right) \right\}$$

335where  $NRMSE_{FM}$  and  $NRMSE_{DM}$  are the normalized root mean square errors for  
336fresh and dry masses respectively. Selected parameters are reported in tables S3  
337and S4.

### 338Model comparison and selection

339On the basis of the best calibration solution, model selection has been performed  
340by comparing measured and simulated cell size distribution, for each model  
341variant. A *semi-quantitative* comparison approach has been used due to the limited  
342experimental information available: the general distribution characteristics (shape,  
343positioning and dispersion) have been characterized rather than a perfect fit. To  
344this aim, 8 descriptive statistical indicators have been computed for each model

345variant and compared to those derived from real- data distribution, namely:

- 346 • skewness and kurtosis (distribution's shape)
- 347 • mean and median cell size (positioning)
- 348 • standard deviation (SD) and median absolute deviation (MAD) (data
- 349 dispersion)
- 350 • maximal and minimal cell size (data dispersion)

351In order to compare different calibration solutions, a *principal component analysis*  
352(PCA) was performed on the descriptors of cell distribution arising from each  
353model estimation. The ade4 library of R software was used for this purpose (R  
354development Core Team 2006).

355

## 356**RESULTS**

357

### 358**A characteristic right-tailed distribution of cell areas**

359

360The distribution of cell sizes at a given stage of fruit development directly  
361depends on the particular cell division and expansion patterns followed by the  
362organ up to the considered time. Any change in the cell division or expansion rate  
363will have a consequence on the shape and position of the observed distribution.  
364For both tomato genotypes considered in this study, the cell area distribution at  
365mature stage shows a typical right-tailed shape (Figure 2), compatible with a  
366Weibull or a Gamma distribution (see section S1). The observed cell sizes span  
367up to two orders of magnitude, with cell areas (cross section) ranging from 0.004  
368to 0.08 mm<sup>2</sup> for Cervil genotype, and from 0.005 to 0.28 mm<sup>2</sup> for Levovil (Table  
3693 and 4). The average cell area is calculated to be 0.026 mm<sup>2</sup> for the cherry  
370tomato and 0.074 mm<sup>2</sup> for the large-fruited genotype, values in agreement with  
371data from other tomato varieties (Bertin, 2005; Renaudin et al., 2017). Data  
372dispersion is higher for the large-fruited genotype, but the shape of the  
373distribution, as measured by its skewness and kurtosis values, is pretty similar for  
374both tomato varieties.

375

376 Assuming that cell area distribution is a good descriptor of the underlying  
377 interaction patterns among cellular processes, a principal component analysis  
378 was performed on 8 statistical descriptors of cell size distribution in order to  
379 compare predictions of M0-M7 models (see M&M and Tables 2 and 3 ). For both  
380 genotypes, the two first principal components explained approximately 90% of  
381 observed variance and were able to correctly separate models with cell-  
382 autonomous control (M0, M5, M6) from models including an organ-wide control  
383 of cell expansion (Figure 3 and 4). For Cervil genotype, the intra-model  
384 variability of cell size distribution was lower than then inter-model differences,  
385 whereas for Levovil models including a ploidy-dependent effect resulted in a  
386 similar cell size distribution.

387

388 Separation was mainly performed by the first principal component on the basis of  
389 the width of the distribution (sd, mad and maximal cell size) and its skewness,  
390 both generally increased in models including an interaction between  
391 endoreduplication-expansion processes (Figure 3 and 4). Models without organ-  
392 wide control are characterized by a reduced dispersion and a larger median  
393 value. With respect to experimental data, models combining an organ-wide and a  
394 ploidy-dependent control gave the best results.

395

396 In the following, the effect of specific control mechanisms on the resulting cell  
397 area distribution is analysed in details, based on the results obtained for the best-  
398 fitting solution. The corresponding statistical descriptors are reported in Table 2  
399 and 3, for Cervil and Levovil genotype respectively. Note that predicted minimal  
400 cell sizes for Levovil genotype are systematically lower than experimental  
401 measurements and correspond to the size of proliferating cells. This is partly due  
402 to the dissociation method employed for cell counting that underestimates small  
403 sub-epidermal cells. These cells although quite numerous contribute little to total  
404 pericarp volume and mass (Renaudin et al., 2017).

405

406 **A simple cell-autonomous control scheme leads to unrealistic cell size**  
407 **distribution**

408

409 As a benchmark model, the case of a simple cell-autonomous control,  
410 without ploidy-dependent effect, was first considered (version M0 of the model).  
411 Accordingly, two cells with the same age, even if initiated at different fruit  
412 developmental stages, behaved identically in what concerns carbon metabolism,  
413 transport and wall mechanical properties. In this scheme, therefore, cell size  
414 variations derived exclusively from the dynamics of cell division, which caused a  
415 shift in the initiation date for different cohort of cells. When applied to our  
416 genotypes, the cell-autonomous model was able to reproduce the observed fruit  
417 mass dynamics but the corresponding cell size distribution was extremely narrow  
418 (Figure 5 A and D), with standard deviation less than  $3e-3$ , and strongly left-tailed  
419 (see Table 2 and 3).

420

421 Including an organ-wide mechanism that controls cell size (model M1)  
422 introduces a source of variance among cells. In this case, two cells of the same  
423 age which were initiated at different fruit stages did *not* behave identically,  
424 resulting in different expansion capabilities and growth patterns (Baldazzi et al.  
425 2013). Following literature information and preliminary studies (Baldazzi et al.,  
426 2017) carbon symplastic transport had been supposed under organ-wide control,  
427 via the progressive closure of plasmodesmata with fruit age (Zambryski,  
428 2004) (see M&M section). As a result, the cell size distribution got larger, and  
429 skewness increased towards zero values, indicating a symmetric cell size  
430 distribution, both for cherry and large-fruited tomatoes. Indeed, the typical right-  
431 tail observed in experimental data was absent and the maximum cell size  
432 predicted by the model was much smaller than expected. This suggested that a  
433 mechanism controlling cell expansion was lacking in the model.

434

435 **Endoreduplication and cell growth: possible interactions and genotypic**

436 **effect**

437

438 A significant correlation between cell size and endoreduplication level has been  
439 often reported. However, the molecular mechanism by which ploidy could

440modulate cell expansion capabilities remain elusive. In this work, three time-  
441dependent cell properties have been selected as possible targets of ploidy-  
442dependent modulation (see M&M section): *a*) the maximum carbon uptake rate  
443(model version M2), *b*) carbon allocation between soluble and non-soluble  
444compounds (model version M3) *c*) cell wall plasticity (model version M4).  
445The three hypotheses were tested independently on both genotypes, in  
446combination with an organ-wide control. Results are shown in Table 2 and 3. In  
447most cases, the addition of a ploidy effect on cell expansion resulted in a positive  
448skewed distribution, with comparable or increased cell size dispersion and  
449maximum cell size with respect to the M0 and M1 models. The strength of the  
450effect however strongly depended on the genotype, with different ranking among  
451model versions.

452

453For Cervil genotype, a potential control of endoreduplication on both the  $V_{max}$   
454(model M2) and cell's allocation strategy (model M3) provided distribution  
455agreement with data, i.e. right-tailed distributions with good dispersion and  
456correct positioning in both mean and median cell area (Figure 5 B and C). The  
457shape of the distribution however was better reproduced by the M2 model, which  
458showed a skewness and kurtosis values close to the observed ones, but the  
459adjustment to fruit growth dynamics, especially for dry mass, was only partially  
460satisfactory (Table 2).

461In both models, a high ploidy level resulted in a larger cell size, although the  
462maximum predicted cell size was slightly lower than the observed one.

463Correlation between ploidy level and cell area was significant with a p-value  
464 $<0.0001$  (Table S5). The heterogeneity of cell sizes usually observed at each  
465ploidy level was correctly captured by the models as a consequence of the  
466asynchrony in cell division and endoreduplication patterns (Bourdon et al., 2011;  
467Roeder et al., 2010). In comparison to the M2 and M3 models, the potential effect  
468of endoreduplication onto cell's mechanical properties (M4) failed to increase cell  
469size variance beyond the values already obtained without any ploidy effect (M1).

470

471For Levovil genotype, the interaction between endoreduplication and expansion

472 had less impact on the resulting cell distribution. For both model M2 and M4, the  
473 addition of a ploidy-dependent effect on cell expansion, although significant, was  
474 not able to produce a right-tailed distribution, as observed in experimental data  
475 (Figure 5E). The shape of the distribution was pretty symmetric, with skewness  
476 values close to zero, reduced dispersion and mean cell size. Only the inclusion of  
477 a ploidy-dependent effect on cell's strategy for carbon allocation (model M3)  
478 allowed increasing the skewness value up to a reasonable value, but the width of  
479 the distribution remained lower than expected with maximal cell sizes not  
480 exceeding 0.13 mm<sup>2</sup> (against the 0.28mm<sup>2</sup> observed) (Figure 5F).

481

482

### 483 **The mechanisms that contribute to cell size variance are likely genotype-** 484 **dependent**

485

486 The above results showed that cell distribution can be significantly affected by  
487 both an organ-wide control of fruit development and a direct interaction between  
488 endoploidy and cell expansion capabilities. In order to better discriminate their  
489 respective role, the effect of a ploidy dependent expansion was tested alone,  
490 without the contribution of an organ-wide control of cell growth (models M5-M7).  
491 Results confirmed that the best results are obtained by a combined action of both  
492 an organ-wide control and a ploidy-dependent modulation of cell expansion but  
493 the relative importance of the two mechanisms is likely genotype-dependent.

494

495 In the case of Levovil, organ-wide control turned out to be a major regulatory  
496 mode. Independently of the interactions between endoreduplication and  
497 expansion, indeed, models without organ-control (models M5-M7) completely  
498 failed to reproduce the observations, resulting in a very narrow and left-tailed cell  
499 size distribution (Table 3). Organ-wide coordination of cell expansion appeared to  
500 be the main responsible for positive skewness of cell size distribution whereas  
501 the addition of an endoreduplication-mediated modulation of cell expansion  
502 capabilities, alone, resulted only in a marginal improvement of model's  
503 performances.

504

505The relative roles of ploidy-dependent and organ-wide control of cell growth  
506appear more balanced in cherry tomatoes. Indeed, with the exception of model  
507M6, both the organ-wide and the ploidy-mediated control of cell expansion were  
508able to reproduce the expected right-tailed distribution shape (Table 2). However,  
509their concomitant action was needed in order to get a realistic cell size variance.  
510The two mechanisms thus seem to act in synergy to increase cell expansion and  
511final cell size.

512

513

514**A combination of ploidy-dependent control of both carbon uptake and**  
515**allocation better explains data**

516

517In spite of a good agreement with pericarp data, all tested models failed to fully  
518reproduce the observed cell area distribution for Levovil genotype. In particular,  
519the maximum reachable cell size predicted by the models was far lower than the  
520observed data. Up to now, for seek of simplicity, interaction between  
521endoreduplication and expansion has been supposed to affect a single process at  
522time but in reality a combination of effects cannot be excluded. We therefore tried  
523to combine a ploidy-dependent effect on both the maximum carbon uptake and  
524the cell's allocation strategy between soluble and non-soluble compounds (model  
525version M23).

526

527Results showed that, for both genotype, the two mechanisms successfully  
528combined together to improve cell's expansion capabilities. As a consequence,  
529the tail of the distribution straightened and the maximal cell size increased  
530towards realistic values (Figure 6). For Cervil genotype, indeed, the predicted cell  
531size distribution approached the experimental one, as showed by the projection of  
532the M23 model onto the first principal plane (Figure 3). For Levovil genotype, in  
533spite of a significant increase of the maximal cell size, the width of the distribution  
534remained much lower than in experimental data, resulting into a very long-tailed  
535distribution shape.

536

537**DISCUSSION**

538

539       The present paper describes an improved version of an integrated cell  
540division-expansion model that explicitly accounts for DNA endoreduplication, an  
541important mechanism in tomato fruit development. The model is used to  
542investigate the interaction among cell division, endoreduplication and expansion  
543processes, in the framework of the neo-cellular theory (Beemster et al., 2003). To  
544this aim, 8 model variants including or not an organ-wide control of cell  
545development, have been tested and compared to data from two contrasting  
546tomato genotypes. Model simulations showed that a pure cellular control was  
547unable to reproduce the observed cell size distribution in terms of both average  
548cell size and cell variance. In agreement with the neo-cellular theory, the model  
549supported the need for an organ-wide control of cell growth, mediated by cell-to-  
550cell communication via plasmodesmata (Han et al., 2014; Norman et al., 2011)  
551and confirmed the role of endoreduplication as an important modulator of the cell  
552expansion potential.

553

554       According to the model, organ-wide control was the main responsible of  
555cell-to-cell variance but a ploidy-mediated effect on cell expansion was needed in  
556order to obtain large cell surface as the ones observed in experimental data. A  
557positive significant correlation between cell size and ploidy level was clearly  
558reproduced, independently of model version, in agreement with recent analysis  
559of cell size in both leaf epidermis (Kawade and Tsukaya, 2017; Roeder et al.,  
5602010) and fruit pericarp (Bourdon et al., 2011).

561

562However, the strength of the correlation may be genotype-dependent. For the  
563cherry tomato variety, our modelling approach showed that a ploidy-dependent  
564control of carbon metabolism (uptake, allocation or a combination of the two), in  
565combination to an organ-wide modulation of cell expansion, was able to generate  
566a cell size distribution close to the observed one. For large-fruited tomato  
567genotype, interaction between endoreduplication and cell expansion via a single  
568process did not suffice to get large cells. Independently of the specific interaction  
569mechanism, the model proved unable to correctly reproduce the observed cell

570 sizes, resulting in a too narrow and symmetric distribution.  
571 The addition of a double effect of cell's endoploidy on both carbon uptake and  
572 allocation was able to increase the maximal cell size close to the correct values,  
573 but dispersion remained lower than expected.

574

#### 575 **Cell stochasticity may be important to explain cell size distribution in fruit**

576

577 A few reasons may account for the discrepancy observed for the large-  
578 fruited variety. A first issue may reside in the quality of experimental data for  
579 Levovil genotype. A rapid computation of the average cell size as the pericarp  
580 volume over the number of cells at maturity, yields a value significantly lower than  
581 the mean of the experimental distribution. This means that the proportion of small  
582 cells is underestimated in our dataset, resulting in a distribution that is probably a  
583 little flatter and less skewed than the real one.

584

585 A second, more fundamental reason of discrepancy is rooted in our modelling  
586 approach. Our model is an example of population model: the fruit is described a  
587 collection of cell groups, each having specific characteristics in terms of number,  
588 mass, age and ploidy level, that dynamically evolve during time. Although  
589 asynchrony in the emergence of cell groups allowed to capture a considerable  
590 part of cell-to-cell heterogeneity, intrinsic stochasticity of cellular processes  
591 (Meyer and Roeder, 2014; Robinson et al., 2011b; Smet and Beeckman, 2011)  
592 are not accounted for. Variations in the threshold size for division (often  
593 associated to a change in the cell cycle duration) as well as asymmetric cell  
594 divisions are considered as important determinant of the final cell size (Dupuy et  
595 al., 2010; Osella et al., 2014; Roeder et al., 2010; Stukalin et al., 2013) they may  
596 contribute to significantly spread the size distribution of both dividing and  
597 expanding cell groups, from the early stages. Moreover, the degree of additional  
598 dispersion introduced by cell expansion is likely to depend on the specificity of the  
599 underlying mechanisms, with possible interactions with ploidy-dependent and  
600 organ-wide controls. Of course, these mechanisms are intrinsic of the  
601 development of any new organ, independently of the genotype, but they can

602prove more sensitive for Levovil genotype than for Cervil in reason of its higher  
603cell number and longer division windows.

604In perspective, the addition of stochastic effects could help to fill the missing  
605variance for both Cervil and Levovil genotypes. To this aim, a novel modelling  
606scheme is needed in which the average cell mass of a group is replaced by a  
607distribution function of cell sizes, whose parameters can evolve with time under  
608the effect of cell expansion processes.

609

### 610**Endoreduplication could regulate cell size through carbon allocation and** 611**metabolism**

612

613 From a biological point of view, the model suggested that  
614endoreduplication may interact with cell's carbon metabolism, increasing the  
615substrate potentially available for cell expansion. This is in line with literature  
616data pointing to ploidy level setting the maximum potential cell size that can be  
617attained or not, depending on internal (hormones) and external (environmental)  
618factors (Breuer et al., 2010; Chevalier et al., 2011; De Veylder et al., 2011). In  
619particular, the model revealed that high ploidy level may increase both the carbon  
620uptake rate and its relative allocation to soluble compounds, thanks to an overall  
621economy in cell wall synthesis (Barow, 2006; Pirrello et al., 2018).

622

623 It is important to stress that the molecular basis of the supposed interaction  
624between endoreduplication and expansion are not described in the model and  
625could involve many molecular players. Moreover, the existence of other targets of  
626a ploidy-dependent control cannot be excluded nor the contribution of other  
627mechanisms to the control of the final cell size. In many fruit species including  
628tomato, a negative correlation between average cell size and cell number has  
629been observed, suggesting the existence of a competition for resources  
630(Lescourret and Génard, 2003; Prudent et al., 2013). This kind of mechanism  
631may contribute to broaden the range of attainable cell sizes, increasing size  
632variance among first and late-initiated cells (see section S5).The importance of  
633such an effect may vary with genotype and environmental conditions (Bertin,

6342005; Quilot and Génard, 2008). This may be especially important for large-  
635fruited tomatoes for which cell number is large.

636

637**Measurement of cell size distribution: promises and challenges to**  
638**understand the control of fruit growth**

639

640 Further work is needed in order to identify the mechanisms behind organ  
641growth and cell size determination. To this aim, the analysis of cell size  
642distribution shows up as a promising approach. When looking at our results,  
643indeed, the NRMSE with respect to pericarp fresh and dry mass was always  
644between 20% and 30% indicating a satisfactory agreement with data,  
645independently from the model version and the tomato genotype. This highlights  
646the fact that the dynamics of fruit growth alone is not enough to discriminate  
647between several biologically-plausible models. In this sense, cell size distribution  
648represents a much more informative dataset as it uniquely results from the  
649specific cell division and expansion patterns of the organ (Halter et al., 2009).

650 The assessment of cell sizes in an organ is not an easy task though. As  
651illustrated by the case of Levovil, the employed measurement technique may  
652have important consequences on the resulting cell size distribution (Legland et  
653al., 2012). Indeed, mechanical constraints acting on real tissues as well as  
654vascularisation can largely modify cell shape, resulting in elongated or multi-lobed  
655cells (Ivakov and Persson, 2013). Thus, if the orientation of 2D slices can  
656potentially affect the resulting cell area estimation, possible differences between  
657*in-vivo* tissues and dissociated cells, both in number and size, should also be  
658checked.

659The use of mutant or modified strains (Musseau et al., 2017) in combination with  
660recent advancements in microscopy and tomography (Mebatsion et al., 2009;  
661Wuyts et al., 2010) could now permit the acquisition of more reliable datasets,  
662opening the way to an in-depth investigation of cell size variance in relation to the  
663their position within the fruit (Renaudin et al., 2017) and to the underlying  
664molecular processes. At term, improvements in the ability of computation models

665to integrate the multiple facets of organ development in a mechanistic way can  
666help to evaluate and quantify the contribution of the different processes to the  
667control of cell growth.

668

669

#### 670**Acknowledgments**

671

672The authors warmly thank B. Brunel for help with cell measurements. The  
673authors are grateful to Inria Sophia Antipolis – Méditerranée "NEF" computation  
674cluster for providing resources and support. This work was partially funded by the  
675Agence Nationale de la Recherche, Project "Frimouss" (grant no. ANR-15-  
676CE20-0009) and by the Agropolis Foundation under the reference ID 1403-032  
677through the « Investissements d'avenir » programme (Labex Agro:ANR-10-LABX-  
6780001-01).

679

680

#### 681**Literature cited**

682

683Asl, L.K., Dhondt, S., Boudolf, V., Beemster, G.T.S., Beeckman, T., Inzé, D.,  
684Govaerts, W., and De Veylder, L. (2011). Model-based analysis of Arabidopsis  
685leaf epidermal cells reveals distinct division and expansion patterns for pavement  
686and guard cells. *Plant Physiol.* *156*, 2172–2183.

687Baldazzi, V., Bertin, N., Genard, M., and Génard, M. (2012). A model of fruit  
688growth integrating cell division and expansion processes. In *Acta Horticulturae*,  
689(International Society for Horticultural Science (ISHS); Leuven; Belgium), pp.  
690191–196.

691Baldazzi, V., Pinet, A., Vercambre, G., Bénard, C., Biais, B., and Génard, M.  
692(2013). In-silico analysis of water and carbon relations under stress conditions. A  
693multi-scale perspective centered on fruit. *Front. Plant Sci.* *4*, 495.

694Baldazzi, V., Génard, M., and Bertin, N. (2017). Cell division, endoreduplication  
695and expansion processes: setting the cell and organ control into an integrated  
696model of tomato fruit development. *Acta Hort.* *1182*.

697Barow, M. (2006). Endopolyploidy in seed plants. *BioEssays* *28*, 271–281.

698Beemster, G.T.S., Fiorani, F., and Inzé, D. (2003). Cell cycle: the key to plant  
699growth control? *Trends Plant Sci.* *8*, 154–158.

700Bertin, N. (2005). Analysis of the tomato fruit growth response to temperature and  
701plant fruit load in relation to cell division, cell expansion and DNA  
702endoreduplication. *Ann. Bot.* *95*, 439–447.

703Bertin, N., Génard, M., and Fishman, S. (2003). A model for an early stage of  
704tomato fruit development: cell multiplication and cessation of the cell proliferative  
705activity. *Ann. Bot.* *92*, 65–72.

706Bertin, N., Lecomte, A., Brunel, B., Fishman, S., and Génard, M. (2007). A model  
707describing cell polyploidization in tissues of growing fruit as related to cessation of  
708cell proliferation. *J. Exp. Bot.* *58*, 1903–1913.

709Boudon, F., Chopard, J., Ali, O., Gilles, B., Hamant, O., Boudaoud, A., Traas, J.,  
710and Godin, C. (2015). A Computational Framework for 3D Mechanical Modeling  
711of Plant Morphogenesis with Cellular Resolution. *PLoS Comput. Biol.* *11*,  
712e1003950.

713Bourdon, M., Coriton, O., Pirrello, J., Cheniclet, C., Brown, S.C., Poujol, C.,  
714Chevalier, C., Renaudin, J.-P.P., and Frangne, N. (2011). In planta quantification  
715of endoreduplication using fluorescent in situ hybridization (FISH). *Plant J.* *66*,  
7161089–1099.

717Breuer, C., Ishida, T., and Sugimoto, K. (2010). Developmental control of  
718endocycles and cell growth in plants. *Curr. Opin. Plant Biol.* *13*, 654–660.

719Bünger-Kibler, S., and Bangerth, F. (1982). Relationship between cell number,  
720cell size and fruit size of seeded fruits of tomato (*Lycopersicon esculentum* Mill.),  
721and those induced parthenocarpically by the application of plant growth  
722regulators. *Plant Growth Regul.* *1*, 143–154.

723Chevalier, C., Nafati, M., Mathieu-Rivet, E., Bourdon, M., Frangne, N., Cheniclet,  
724C., Renaudin, J.-P., Gévaudant, F., and Hernould, M. (2011). Elucidating the  
725functional role of endoreduplication in tomato fruit development. *Ann. Bot.* *107*,  
7261159–1169.

727Chevalier, C., Bourdon, M., Pirrello, J., Cheniclet, C., Gévaudant, F., Frangne, N.,  
728Gévaudant, F., and Frangne, N. (2014). Endoreduplication and fruit growth in  
729tomato: evidence in favour of the karyoplasmic ratio theory. *J. Exp. Bot.* *65*, 1–16.

730Constantinescu, D., Memmah, M.-M., Vercambre, G., Génard, M., Baldazzi, V.,

731Causse, M., Albert, E., Brunel, B., Valsesia, P., and Bertin, N. (2016). Model-  
732Assisted Estimation of the Genetic Variability in Physiological Parameters Related  
733to Tomato Fruit Growth under Contrasted Water Conditions. *Front. Plant Sci.* 7,  
7341–17.

735Crawford, K.M., and Zambryski, P.C. (2001). Non-targeted and targeted protein  
736movement through plasmodesmata in leaves in different developmental and  
737physiological states. *Plant Physiol.* 125, 1802–1812.

738Dupuy, L., Mackenzie, J., and Haseloff, J. (2010). Coordination of plant cell  
739division and expansion in a simple morphogenetic system. *Proc. Natl. Acad. Sci.*  
740U. S. A. 107, 2711–2716.

741Edgar, B.A., Zielke, N., and Gutierrez, C. (2014). Endocycles: a recurrent  
742evolutionary innovation for post-mitotic cell growth. *Nat. Rev. Mol. Cell Biol.* 15,  
743197–210.

744Fanwoua, J., De Visser, P.H.B., Heuvelink, E., Yin, X., Struik, P.C., and Marcelis,  
745L.F.M. (2013). A dynamic model of tomato fruit growth integrating cell division, cell  
746growth and endoreduplication. *Funct. Plant Biol.* 40, 1098.

747Ferjani, A., Horiguchi, G., Yano, S., and Tsukaya, H. (2007). Analysis of leaf  
748development in fugu mutants of *Arabidopsis* reveals three compensation modes  
749that modulate cell expansion in determinate organs. *Plant Physiol.* 144, 988–999.

750Fishman, S., and Génard, M. (1998). A biophysical model of fruit growth:  
751simulation of seasonal and diurnal dynamics of mass. *Plant Cell Env.* 21, 739–  
752752.

753Fleming, A.J. (2006). The integration of cell proliferation and growth in leaf  
754morphogenesis. *J. Plant Res.* 119, 31–36.

755Halter, M., Elliott, J.T., Hubbard, J.B., Tona, A., and Plant, A.L. (2009). Cell  
756volume distributions reveal cell growth rates and division times. *J. Theor. Biol.*  
757257, 124–130.

758Han, X., Kumar, D., Chen, H., Wu, S., and Kim, J.-Y. (2013). Transcription factor-  
759mediated cell-to-cell signalling in plants. *J. Exp. Bot.*

760Han, X., Kumar, D., Chen, H., Wu, S., and Kim, J.Y. (2014). Transcription factor-  
761mediated cell-to-cell signalling in plants. *J. Exp. Bot.* 65, 1737–1749.

762Horiguchi, G., and Tsukaya, H. (2011). Organ Size Regulation in Plants: Insights  
763from Compensation. *Front. Plant Sci.* 2, 24.

764Ivakov, A., and Persson, S. (2013). Plant cell shape: modulators and  
765measurements. *Front. Plant Sci.* *4*, 439.

766John, P.C.L., and Qi, R. (2008). Cell division and endoreduplication: doubtful  
767engines of vegetative growth. *Trends Plant Sci.* *13*, 121–127.

768Kawade, K., and Tsukaya, H. (2017). Probing the stochastic property of  
769endoreduplication in cell size determination of *Arabidopsis thaliana* leaf epidermal  
770tissue. *PLoS One* *12*, e0185050.

771Kawade, K., Horiguchi, G., and Tsukaya, H. (2010). Non-cell-autonomously  
772coordinated organ size regulation in leaf development. *Development* *137*, 4221–  
7734227.

774Kuchen, E.E., Fox, S., de Reuille, P.B., Kennaway, R., Bensmihen, S., Avondo, J.,  
775Calder, G.M., Southam, P., Robinson, S., Bangham, A., et al. (2012). Generation  
776of leaf shape through early patterns of growth and tissue polarity. *Science* *335*,  
7771092–1096.

778Lee, H.-C., Chen, Y.-J., Markhart, A.H., and Lin, T.-Y. (2007). Temperature effects  
779on systemic endoreduplication in orchid during floral development. *Plant Sci.* *172*,  
780588–595.

781Legland, D., Devaux, M.-F., Bouchet, B., Guillon, F., and Lahaye, M. (2012).  
782Cartography of cell morphology in tomato pericarp at the fruit scale. *J. Microsc.*  
783*247*, 78–93.

784Lescourret, F., and Génard, M. (2003). A multi-level theory of competition for  
785resources applied to fruit production. *Écoscience* *10*, 334–341.

786Liu, H.-F.F.H.-F., Génard, M., Guichard, S., and Bertin, N. (2007). Model-assisted  
787analysis of tomato fruit growth in relation to carbon and water fluxes. *J. Exp. Bot.*  
788*58*, 3567–3580.

789Löfke, C., Dünser, K., Scheuring, D., Kleine-Vehn, J., Barbez, E., Kubeš, M.,  
790Rolčik, J., Béziat, C., Pěnčík, A., Wang, B., et al. (2015). Auxin regulates SNARE-  
791dependent vacuolar morphology restricting cell size. *Elife* *4*, 119–122.

792Lucas, M., Kenobi, K., von Wangenheim, D., Voß, U., Swarup, K., De Smet, I.,  
793Van Damme, D., Lawrence, T., Péret, B., Moscardi, E., et al. (2013). Lateral root  
794morphogenesis is dependent on the mechanical properties of the overlaying  
795tissues. *Proc. Natl. Acad. Sci. U. S. A.* *110*, 5229–5234.

796Mebatsion, H.K., Verboven, P., Melese Endalew, A., Billen, J., Ho, Q.T., and

797Nicolaï, B.M. (2009). A novel method for 3-D microstructure modeling of pome  
798fruit tissue using synchrotron radiation tomography images. *J. Food Eng.* 93,  
799141–148.

800Melaragno, J., Mehrotra, B., and Coleman, A. (1993). Relationship between  
801endopolyploidy and cell size in epidermal tissue of Arabidopsis. *Plant Cell Online*  
8025, 1661–1668.

803Musseau, C., Just, D., Jorly, J., G?vaudant, F., Moing, A., Chevalier, C., Lemaire-  
804Chamley, M., Rothan, C., and Fernandez, L. (2017). Identification of Two New  
805Mechanisms That Regulate Fruit Growth by Cell Expansion in Tomato. *Front.*  
806*Plant Sci.* 8, 1–15.

807Norman, J.M. Van, Breakfield, N.W., Benfey, P.N., Carolina, N., Van Norman,  
808J.M., Breakfield, N.W., and Benfey, P.N. (2011). Intercellular communication  
809during plant development. *Plant Cell* 23, 855–864.

810Okello, R.C.O., Heuvelink, E., de Visser, P.H.B., Struik, P.C., and Marcelis, L.F.M.  
811(2015). What drives fruit growth? *Funct. Plant Biol.* 42, 817.

812Osella, M., Nugent, E., and Cosentino Lagomarsino, M. (2014). Concerted control  
813of *Escherichia coli* cell division. *Proc. Natl. Acad. Sci. U. S. A.* 111, 4–8.

814Pirrello, J., Deluche, C., Frangne, N., Gévaudant, F., Maza, E., Djari, A., Bourge,  
815M., Renaudin, J.-P., Brown, S., Bowler, C., et al. (2018). Transcriptome profiling of  
816sorted endoreduplicated nuclei from tomato fruits: how the global shift in  
817expression ascribed to DNA ploidy influences RNA-Seq data normalization and  
818interpretation. *Plant J.* 93, 387–398.

819Proseus, T.E., and Boyer, J.S. (2006). Identifying cytoplasmic input to the cell wall  
820of growing *Chara corallina*. *J. Exp. Bot.* 57, 3231–3242.

821Proseus, T.E., Ortega, J.K.E., and Boyer, J.S. (1999). Separating Growth from  
822Elastic Deformation during Cell Enlargement. *Plant Physiol.* 119, 775–784.

823Prudent, M., Dai, Z.W., Génard, M., Bertin, N., Causse, M., and Vivin, P. (2013).  
824Resource competition modulates the seed number-fruit size relationship in a  
825genotype-dependent manner: A modeling approach in grape and tomato. *Ecol.*  
826*Modell.*

827Quilot, B., and Génard, M. (2008). Is competition between mesocarp cells of  
828peach fruits affected by the percentage of wild species ( *Prunus davidiana* )  
829genome? *J. Plant Res.* 121, 55–63.

830Renaudin, J.-P., Deluche, C., Cheniclet, C., Chevalier, C., and Frangne, N.  
831(2017). Cell layer-specific patterns of cell division and cell expansion during fruit  
832set and fruit growth in tomato pericarp. *J. Exp. Bot.* *68*, 1613–1623.

833Rewers, M., Sadowski, J., and Sliwinska, E. (2009). Endoreduplication in  
834cucumber (*Cucumis sativus*) seeds during development, after processing and  
835storage, and during germination. *Ann. Appl. Biol.* *155*, 431–438.

836Robinson, S., Barbier de Reuille, P., Chan, J., Bergmann, D., Prusinkiewicz, P.,  
837and Coen, E. (2011). Generation of spatial patterns through cell polarity  
838switching. *Science* (80-. ). *333*, 1436–1440.

839Roeder, A.H.K., Chickarmane, V., Cunha, A., Obara, B., Manjunath, B.S., and  
840Meyerowitz, E.M. (2010). Variability in the control of cell division underlies sepal  
841epidermal patterning in *Arabidopsis thaliana*. *PLoS Biol.* *8*, e1000367.

842Sablowski, R., and Carnier Dornelas, M. (2014). Interplay between cell growth  
843and cell cycle in plants. *J. Exp. Bot.* *65*, 2703–2714.

844Serrano-Mislata, A., Schiessl, K., and Sablowski, R. (2015). Active Control of Cell  
845Size Generates Spatial Detail during Plant Organogenesis. *Curr. Biol.* *25*, 2991–  
8462996.

847Stukalin, E.B., Aifuwa, I., Kim, J.S., Wirtz, D., and Sun, S.X. (2013). Age-  
848dependent stochastic models for understanding population fluctuations in  
849continuously cultured cells. *J. R. Soc. Interface* *10*, 20130325.

850Sugimoto-Shirasu, K., and Roberts, K. (2003). “Big it up”: endoreduplication and  
851cell-size control in plants. *Curr. Opin. Plant Biol.* *6*, 544–553.

852Tsukaya, H. (2003). Organ shape and size: a lesson from studies of leaf  
853morphogenesis. *Curr. Opin. Plant Biol.* *6*, 57–62.

854De Veylder, L., Larkin, J.C., and Schnittger, A. (2011). Molecular control and  
855function of endoreplication in development and physiology. *Trends Plant Sci.* *16*,  
856624–634.

857von Wangenheim, D., Fangerau, J., Schmitz, A., Smith, R.S., Leitte, H., Stelzer,  
858E.H.K., and Maizel, A. (2016). Rules and Self-Organizing Properties of Post-  
859embryonic Plant Organ Cell Division Patterns. *Curr. Biol.* *26*, 439–449.

860Wuyts, N., Palauqui, J.-C., Conejero, G., Verdeil, J.-L., Granier, C., and  
861Massonnet, C. (2010). High-contrast three-dimensional imaging of the  
862*Arabidopsis* leaf enables the analysis of cell dimensions in the epidermis and

863mesophyll. *Plant Methods* 6, 17.

864Zambryski, P.C. (2004). Cell-to-cell transport of proteins and fluorescent tracers  
865via plasmodesmata during plant development. *J. Cell Biol.* 164, 165–168.

866

867

868

869

870

871

872

873

874

875

876

877

878

879

880

881

882

883

#### 884**Figures**

885

886

887Figure 1: Scheme of the integrated model. The fruit is described as a collection of cell populations,  
888each one having a specific age, ploidy and volume. Cells can be either proliferating or expanding-  
889endoreduplicating. The number of cells in each class is predicted by the division-  
890endoreduplication module, assuming a progressive decline of cells' proliferating activity.  
891Expanding cells grow according to the expansion module which provides a biophysical description  
892of the main processes involved in carbon and water accumulation. It is assumed that the onset of  
893endoreduplication coincides with the beginning of the expansion phase. Two timescales are  
894recognizable in the model: the organ age i.e. the time since the beginning of the simulation, and  
895the cell age i.e. the time since the cell left the mitotic cycle and entered the expansion-  
896endoreduplication phase. Depending on the model version, cell expansion may be modulated by  
897organ age (organ-wide control) and/or by cell's ploidy.

898

899

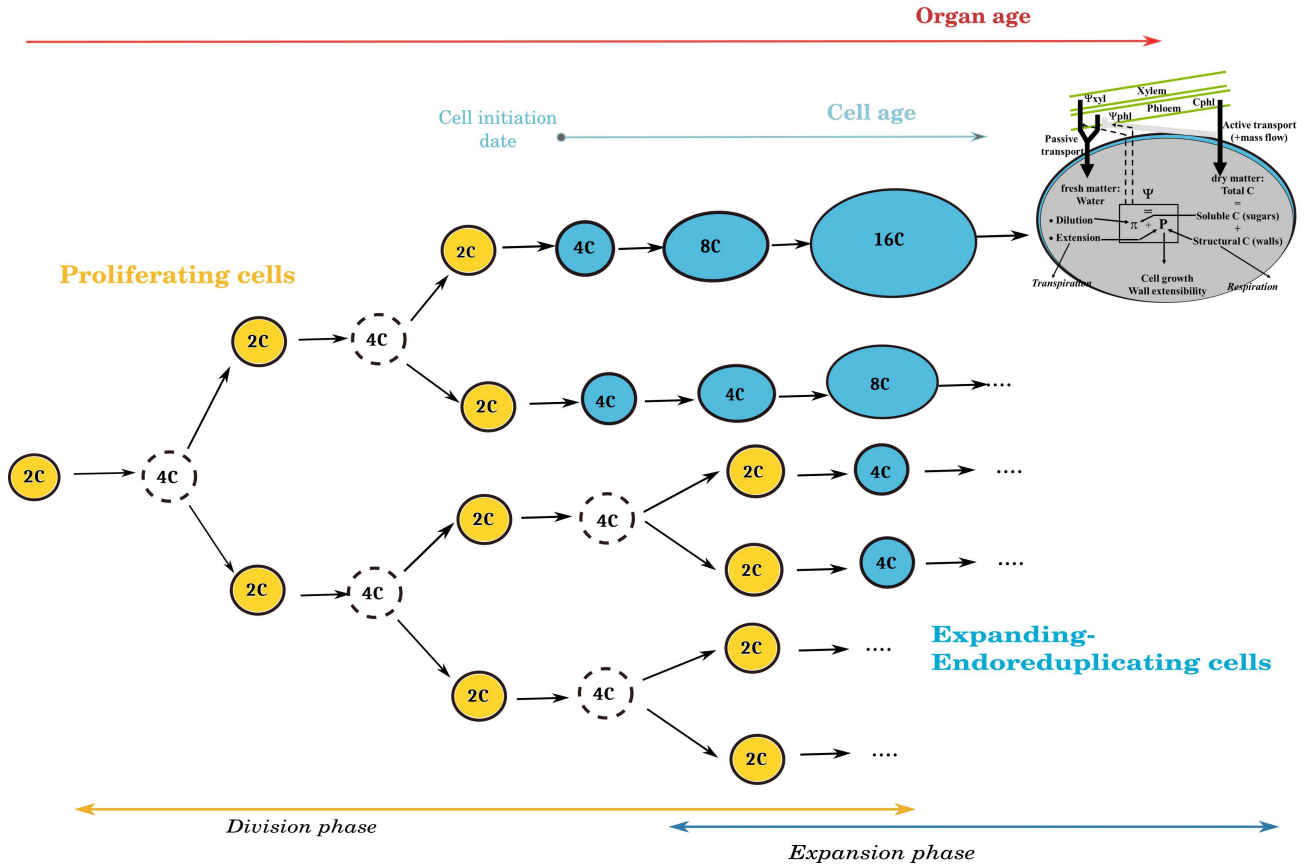
900

901

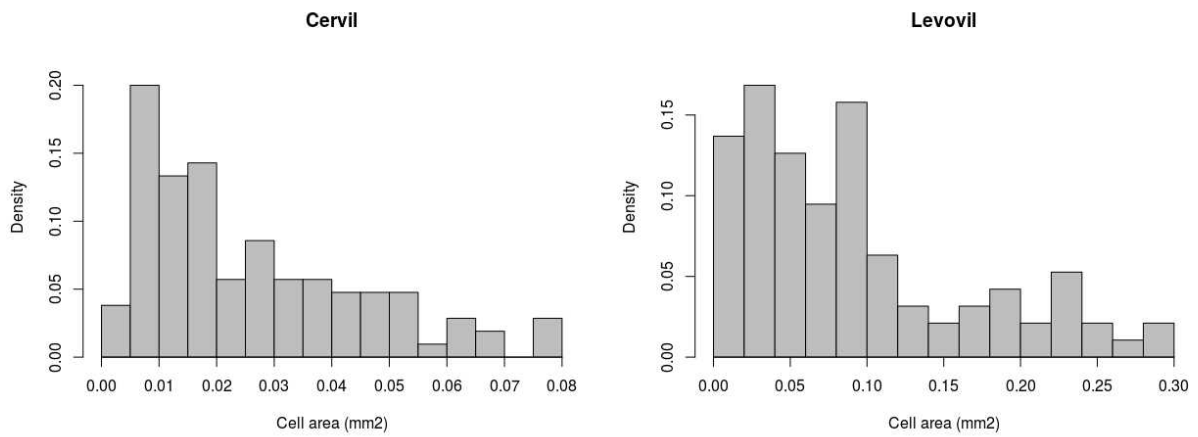
902

903

904



906



908 Figure 2: Measured cell size distribution at fruit maturity Left: Cervil genotype. Right: Levovil

909 genotype.

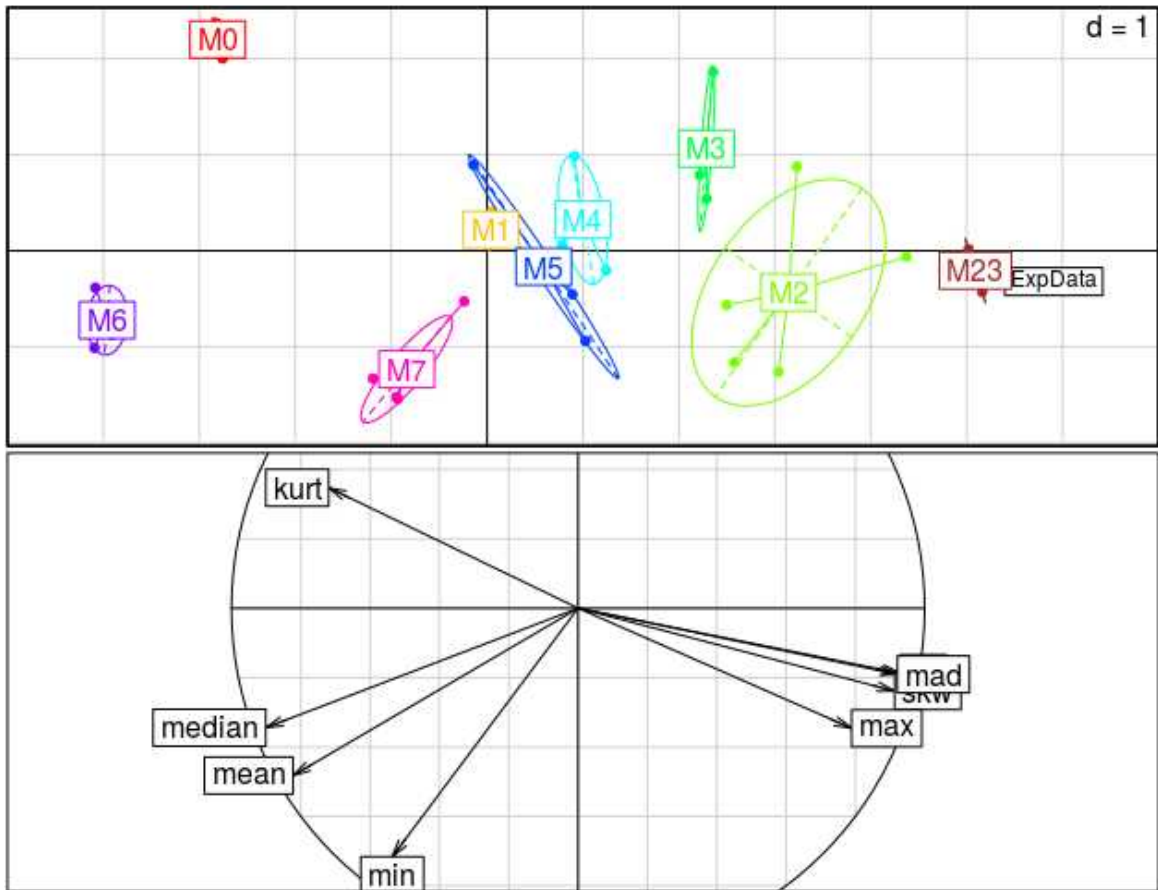
910

911

912

913

914  
 915  
 916  
 917  
 918  
 919  
 920  
 921  
 922  
 923  
 924  
 925  
 926  
 927  
 928  
 929  
 930  
 931  
 932  
 933  
 934  
 935



937

938

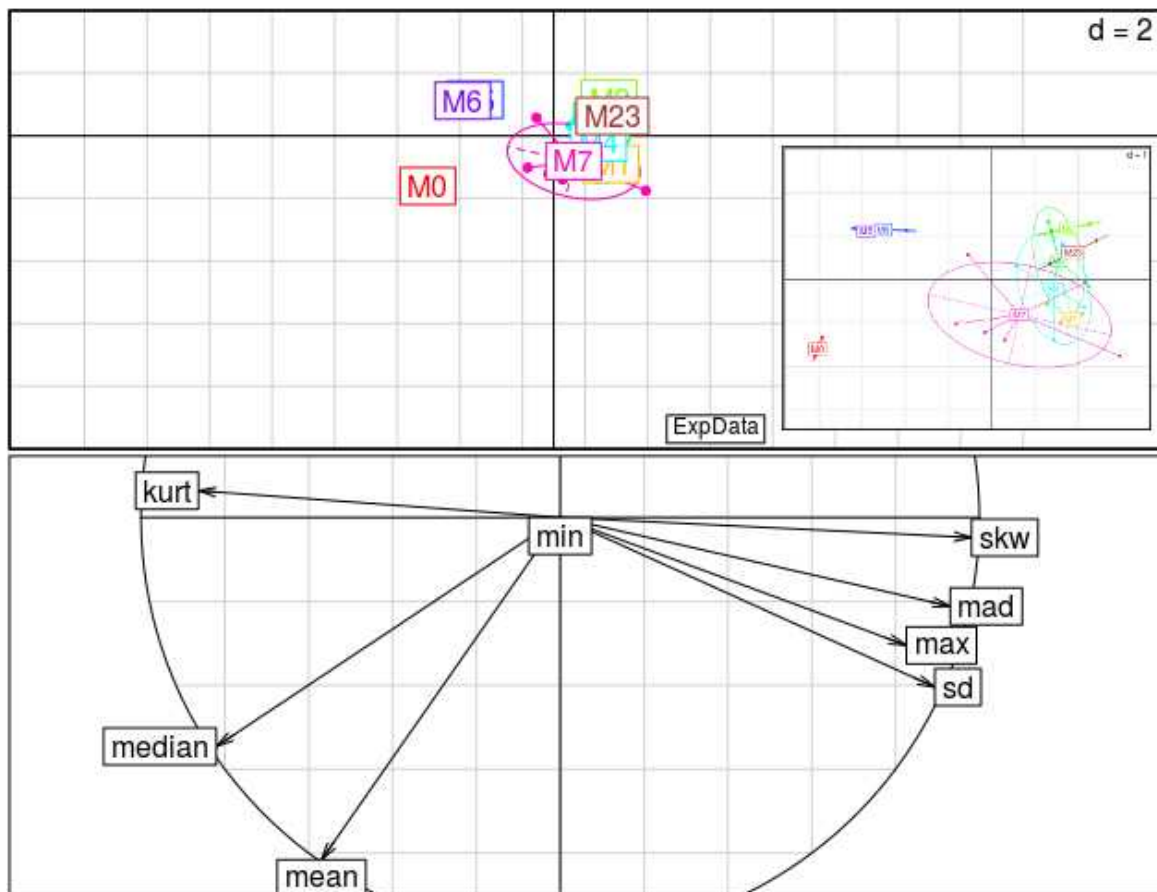
939Figure 3: Principal component analysis (PCA) cell size distributions obtained for the different  
940estimations of models M0-M7 on Cervil genotype. 8 statistical descriptors are used as variables to  
941characterize cell distribution. Measured cell size distribution results of model M23 are projected  
942as a supplementary observation. *Top*: Projection of individual distributions on the PC1-PC2 plane.  
943Model variants are tagged with different colors. *Bottom*: Correlation of the variables with the first  
944two principal components.

945

946

947

948



950

951Figure 4: Principal component analysis (PCA) cell size distributions obtained for the different  
952estimations of models M0-M7 on Levovil genotype. 8 statistical descriptors are used as variables  
953to characterize cell distribution. Measured cell size distribution and results of model M23 are  
954projected as a supplementary observation. *Top*: Projection of individual distributions on the PC1-  
955PC2 plane. Model variants are tagged with different colors. *Bottom*: Correlation of the variables  
956with the first two principal components.

957  
 958  
 959  
 960  
 961  
 962  
 963  
 964  
 965  
 966  
 967  
 968  
 969  
 970  
 971  
 972  
 973  
 974  
 975  
 976  
 977  
 978  
 979  
 980  
 981

Figure 5: Predicted cell area distribution at fruit maturity. On the left side, Cervil genotype: A: model M0, B: model M2, C: model M3. On the right side, Levovil genotype: D: model M0, E: model M2, F: model M3.

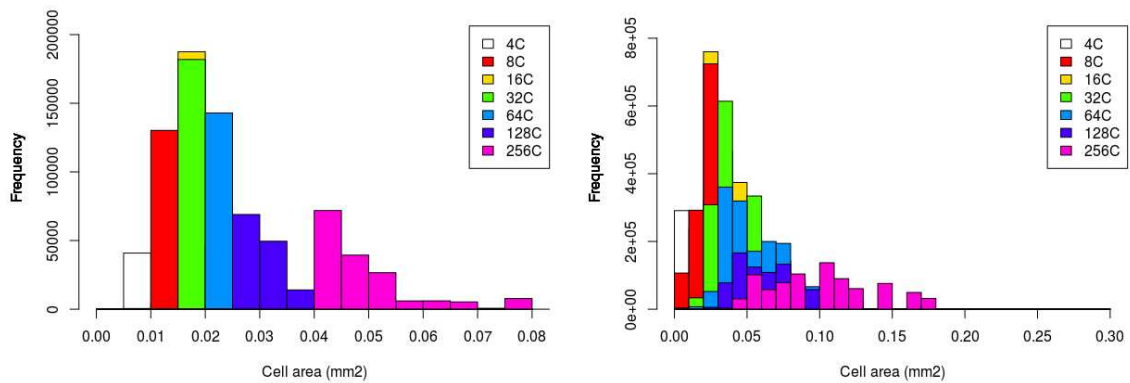
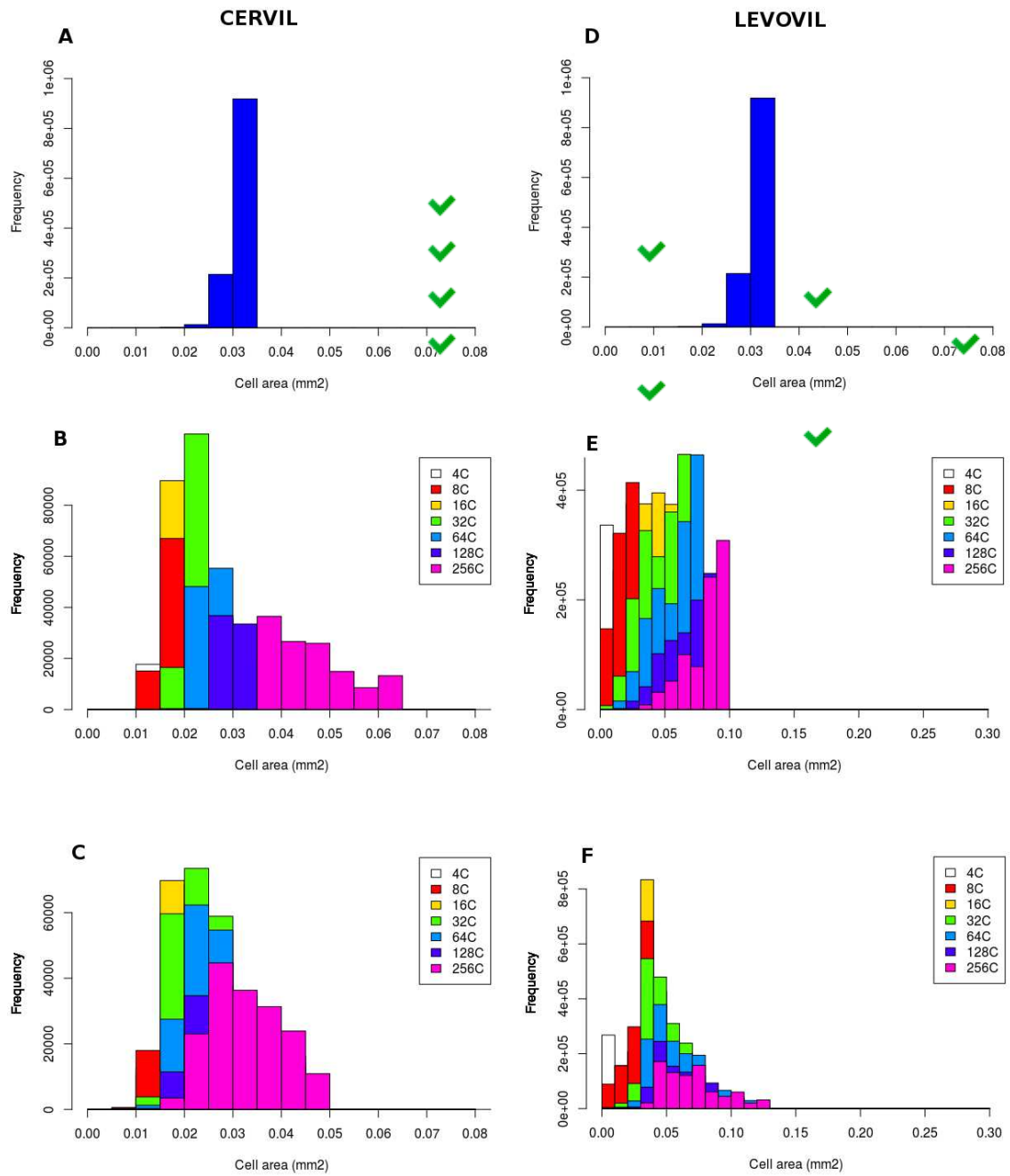


Figure 6: Predicted cell area distribution at fruit maturity for model M23, combining a ploidy-dependent effect on both carbon uptake and allocation. Left: Cervil genotype. Right: Levovil genotype.

985  
 986  
 987

**988 Tables**

989



991

992 Table 1: Experimental design showing the characteristics of the 8 model versions tested

993 in the paper.

994

995

996

997

998

999  
 1000  
 1001  
 1002  
 1003  
 1004  
 1005  
 1006  
 1007  
 1008  
 1009  
 1010  
 1011  
 1012  
 1013  
 1014  
 1015

MODEL	FRUIT MASS		CELL DISTRIBUTION							
	FIT QUALITY		SHAPE		POSITIONING				DISPERSION	
	NRMSE FM	NRMSE DM	Skewness	Kurtosis	Mean	Median	Min	Max	SD	MAD
<b>Exp Data</b>			<b>0.97</b>	<b>3.13</b>	<b>0.026</b>	<b>0.019</b>	<b>0.0039</b>	<b>0.08</b>	<b>0.019</b>	<b>0.016</b>
M0	31.49	31.34	-4.06	30.34	0.030	0.031	0.0042	0.033	0.0015	0.0005
M1	28.32	29.58	0.42	3.07	0.030	0.029	0.0044	0.041	0.0046	0.0042
M2	23	36	0.98	3.58	0.027	0.025	0.0035	0.062	0.011	0.0099
M3	20.18	31.24	0.53	2.58	0.026	0.025	0.0033	0.046	0.0077	0.008
M4	24.97	27.73	0.53	3.45	0.027	0.027	0.0040	0.045	0.005	0.005
M5	34.35	37.02	0.33	3.44	0.029	0.029	0.0040	0.037	0.0035	0.003
M6	34.21	33.81	-3.7	24.9	0.036	0.036	0.0051	0.039	0.002	0.0008
M7	29.53	32.47	0.24	3.34	0.034	0.033	0.0040	0.056	0.005	0.005
M23	23.33	33.05	2.0	8.9	0.026	0.021	0.0037	0.11	0.015	0.009

1016  
 1017Table 2 Statistical descriptors for the measured and predicted cell area distribution for Cervil  
 1018genotype. The NRMSE scores for predicted pericarp dry and fresh masses corresponding to the  
 1019selected solution are reported under the columns "Fit Quality". For an easier interpretation, green  
 1020boxes indicate an agreement within 30% with respect to experimental data, yellow an agreement  
 1021between 30 and 40%, white between 40% and 70% and red a strong discrepancy (over 70%  
 1022difference with respect to data).

1023  
 1024  
 1025  
 1026

1027  
 1028  
 1029  
 1030  
 1031  
 1032  
 1033  
 1034  
 1035  
 1036  
 1037  
 1038  
 1039  
 1040  
 1041

MODEL	FRUIT MASS		CELL DISTRIBUTION							
	FIT QUALITY		SHAPE		POSITIONING				DISPERSION	
	NRMSE FM	NRMSE DM	Skewness	Kurtosis	Mean	Median	Min	Max	SD	MAD
<b>Exp Data</b>			<b>0.99</b>	<b>3.01</b>	<b>0.092</b>	<b>0.074</b>	<b>0.0048</b>	<b>0.28</b>	<b>0.075</b>	<b>0.063</b>
M0	23.3	25.27	-2.37	7.89	0.069	0.077	0.00049	0.078	0.017	0.0023
M1	25.79	25.32	0.26	2.13	0.059	0.052	0.00049	0.12	0.030	0.034
M2	25.39	25.59	-0.075	2.2	0.047	0.043	0.00049	0.12	0.022	0.017
M3	25.77	25.01	0.67	3.74	0.047	0.043	0.00049	0.13	0.022	0.017
M4	23.64	25.23	-0.15	2.8	0.053	0.054	0.00049	0.11	0.022	0.020
M5	23.36	27.47	-1.51	5.85	0.054	0.056	0.00049	0.077	0.014	0.008
M6	23.61	25.15	-2.22	7.31	0.055	0.060	0.00049	0.066	0.013	0.004
M7	23.74	25.42	-0.56	3.41	0.063	0.066	0.00049	0.10	0.020	0.018
M23	25.45	28.20	1.46	5.73	0.047	0.039	0.00049	0.018	0.028	0.021

1042  
 1043Table 3: Statistical descriptors for the measured and predicted cell area distribution for Levovil  
 1044genotype. The NRMSE scores for predicted pericarp dry and fresh masses corresponding to the  
 1045selected solution are reported under the columns “Fit Quality”. For an easier interpretation, green  
 1046boxes indicate an agreement within 30% with respect to experimental data, yellow an agreement  
 1047between 30 and 40%, white between 40% and 70% and red a strong discrepancy (over 70%  
 1048difference with respect to data).  
 1049  
 1050